JTTEE5 21:975–986
DOI: 10.1007/s11666-012-9770-1
1059-9630/$19.00 © ASM International

Performance of Detonation Gun-Sprayed Ni-20Cr Coating on ASTM A213 TP347H Steel in a Boiler Environment

G. Kaushal, H. Singh, and S. Prakash

(Submitted November 21, 2011; in revised form February 13, 2012)

Detonation gun-sprayed coatings are known for their high density, high bond strength, moderate substrate heating, superior surface finish, better wear/corrosion resistance, and low cost. In this study, detonation gun-spraying technique was used to deposit Ni-20Cr coating on a commonly used boiler steel ASTM A213 TP347H. The specimens with and without coating were subjected to cyclic oxidation testing at an elevated temperature of 700 °C in actual boiler environment to ascertain the usefulness of the coating. The mass change technique was used to establish the kinetics of erosion-corrosion. XRD and SEM/EDS techniques were used to analyze the exposed samples. The uncoated sample suffered from erosion, and a significant mass loss was recorded. It was observed that overall mass loss was reduced by 83% and thickness loss by 53% after the application of the coating. The detonation gun-sprayed Ni-20 Cr coating was found to be suitable to impart erosion resistance to the given steel in the actual boiler environment.

Keywords boiler environment, D-Gun, erosion-corrosion, high-temperature oxidation, protective coating

1. Introduction

The conventional boilers, where various grades of stainless steel are used as the base materials for their tubes, face the acute problem of degradation by high-temperature oxidation of hot-section components, which is accompanied by erosion as well (Ref 1-6). The atmosphere in power plant boilers has a sufficient free oxygen content to account for a combined erosion-corrosion (E-C) process, consisting of an oxidizing gas at elevated temperature carrying erosive fly ash which impact against metallic surfaces (Ref 7). The combination of high temperatures with contaminants of environment and low-grade fuels, such as sodium, sulfur, vanadium, and chlorine, require special attention to the phenomenon of high-temperature corrosion. This form of corrosion consumes the material unpredictably at very rapid rate (Ref 8). Oxidation and high-temperature corrosion resistance of these materials used in the high-temperature regions is improved by the application of protective coatings. Thermal spray coating can be applied to overcome the oxidation/corrosion problems since it alters the surface without affecting the bulk material properties (Ref 9-12). These coatings can offer an alternative to diffusion coatings. Although protective surface treatments are widely used at low temperature, the application of these at elevated temperature is relatively recent. Detonation gun (D-Gun) spraying, developed in the late quarter of the 1900s, owns the same virtues as the other thermal spraying processes and gives a wide range for the coating materials (Ref 13). Furthermore, D-Gun-spraying process can get the top temperature as high as 3850 °C in the combustion, and accelerate powder particles to a speed of 600-1200 m/s, which is much higher than that of low-pressure plasma spraying (about 400 m/s) and High-Velocity Oxy-Fuel (HVOF) spraying (at maximum 500 m /s) (Ref 13). As a result, the detonation-sprayed coating gets a denser microstructure. Its surface hardness and adhesion strength are usually higher in comparison to other thermal spray coatings such as plasma spray and HVOF sprayed coatings.

Power plants are one of the major industries suffering from severe E-C problems resulting in the substantial losses. According to a survey (Ref 14) conducted over a period of 12 years, encompassing 413 investigations, overheating was listed as the cause of 201 failures or 48.7% of those investigated. Fatigue and corrosion fatigue were listed as the next most common causes of failure accounting for a total of 89 failures or 21.5%. Corrosion, stress corrosion, and hydrogen embrittlement caused a total of 68 failures or 16.5%. In another case study of a coal-fired boiler of a power plant in north western region of India, Prakash et al. (Ref 15) have reported that out of 89 failures occurring in one-year duration, 50 failures were found to be due to hot-corrosion and erosion by ash. Sullivan et al. (Ref 16) reported that the maximum forced

G. Kaushal, RIMT-Institute of Engineering & Technology Mandi Gobindgarh, Punjab, India; **H. Singh**, Indian Institute of Technology Ropar, Rupnagar, Punjab, India; and **S. Prakash**, Indian Institute of Technology Roorkee, Roorkee, Uttarakhand, India. Contact e-mails: gagankaushal@yahoo.com and gagankaushal@rimt.ac.in.

outages in all types of boilers are caused by tube failures. These facts endorse the need to devise some means to control the corrosion/erosion of power plant boilers. The concern to develop and investigate the performance of various coating compositions for power plant boilers has always been a major area of research. Considerable research has been done to evaluate the performance of HVOF- and D-Gun-sprayed coatings in air and salt environments under laboratory conditions, especially of the former. However, it is learnt from the literature that further research is still needed to investigate the performance of these coatings in some newer and more aggressive boiler environments, which may be simulated in the laboratory or in actual industrial conditions. It has also been learnt that there is a further need to develop high-performance coating compositions to be deposited by thermal spray processes for various industrial applications especially for the power plant boilers. In an earlier publication (Ref 17), the authors have presented a comparative performance of HVOF and D-Gun-sprayed Ni-20Cr coatings on ASTM-SAE 213-T22 steel in an actual boiler environment and found that HVOF-sprayed Ni-20Cr coating outperformed D-Gun-sprayed Ni-20Cr coating. The aim of the current investigation is to explore the possibility of deposition of Ni-20Cr coatings on a boiler steel ASTM A213 TP347H (347H) by D-Gun spraying and to study its in-depth performance in an actual boiler under cyclic E-C conditions. Cyclic conditions have been chosen because they resemble actual industrial situations. The steel selected is used extensively for the power plant boiler components mainly in the superheater zone where it has been observed that it suffers from high-temperature E-C by fly ash particles. The outcome of the study will be useful to explore the possibility of use of this coating-process system for the power plant boilers.

2. Experimental Procedure

2.1 Development of Coatings

2.1.1 Substrate Material. The 347H boiler steel tube material with chemical composition: C—0.04-0.1, Mn—2.0, P—0.04 max, S—0.03 max, Si—0.75 max, Cr—17-19, Ni—9.0-13, and Fe—65.08 (mass%) has been used as a substrate material in the current study. The specimens each measuring 20 mm × 15 mm × 5 mm approximately were cut from the fresh boiler tubes.The specimens were polished down to 180 grit SiC paper finish and were grit blasted with Al_2O_3 (grit 60) before the deposition of the coating.

2.1.2 Coating Formulation. The Ni-20Cr was coated on the steel samples using the commercially available D-gun-spraying process at M/S Sai Surface Coating Technologies, Hyderabad, India. The flame temperature was 3900 °C, and maximum spray rate was 3 kg/h. The gas flow rate was 11 m^3/h, and particle impact velocity was 600-1200 m/s. The D-Gun-spraying process parameters have been reproduced in Table 1 (Ref 18).

Table 1 Process parameters employed for the D-Gun spraying (Ref 18)

Parameter	Related value
Oxygen flow rate, kg/cm^2	2640
C_2H_2 flow rate, kg/cm^2	2240
N_2 flow rate, kg/cm^2	960
Spray distance, mm	140
Frequency of shots, s	3

2.2 Characterization of As-Sprayed Coating

The as-sprayed coating was examined visually. Apparent surface porosity of the as-sprayed Ni-20Cr coating was measured by Image analyzer system from Chennai Metco Pvt. Ltd. (India) using Envision 3.0 software based on ASTM 276. The images were obtained through the attached inverted metallurgical microscope. Image analysis of 10 fields on the surface of each coated sample produced the value of the average porosity reported. X-ray diffraction (XRD) analysis of the coated samples was carried out using a Bruker AXS D-8 Advance Diffractometer (Germany) with CuKα radiation and nickel filter at 20 mA under a voltage of 35 kV. The specimens were scanned with a scanning speed of 1 kcps in the 2θ range of 10°-110° and the intensities were recorded at a chart speed of 1 cm/min with 2°/min as Goniometer speed. The diffractometer interfaced with the Bruker DIFFRAC Plus X-Ray diffraction software provided the "*d*" values directly on the diffraction pattern. Field-emission-scanning electron microscopy/energy dispersive spectroscopy (FE-SEM/EDS) analysis (FE-SEM, FEI, Quanta 200F) was performed to characterize the surface morphology of the coating. After the surface characterization, the samples were sectioned, mounted in epoxy powder by using hot mounting method. The mounting was done on a hydraulic mounting machine (Bain mount, Chennai Metco Ltd., India). The mounted specimens were further subjected to polishing, using emery papers of 220, 400, 600 grit and subsequently 1/0, 2/0, 3/0 and 4/0 grades. Fine polishing was carried out to obtain a mirror finish using a 0.3-μm diamond paste. The polished samples were characterized to obtain their cross-sectional morphology and compositions by the FE-SEM/EDS analysis. The EDS Genesis software was used to calculate the composition of the elements in the samples from their corresponding emitted x-ray peaks. X-ray mappings of the various elements were also taken by the same FE-SEM/EDS machine.

2.3 E-C Studies in Actual Environment

Both the coated, as well as, uncoated samples were subjected to the actual boiler in the low temperature primary superheater (LTSH) zone of Guru Gobind Singh Super Thermal Power Plant, Ropar, Punjab, India. The chemical analysis of the ash inside the said boiler has been reproduced in Table 2 (Ref 19) and that of flue gas in Table 3 (Ref 19). The chemical analysis of Indian coal used in the boiler is shown in Table 4. The specimens were

Table 2 Chemical analysis of ash deposited in the boiler (Ref 19)

Constituent	Mass%
Silica	54.7
Fe_2O_3	5.18
Al_2O_3-Fe_2O_3/Al_2O_3	29.56
CaO	1.48
MgO	1.45
SO_3	0.23
Na_2O	0.34
K_2O	1.35
Ignition loss	4.31

Table 3 Chemical analysis of flue gas present in the boiler (Ref 19)

Constituent value	Related
Volumetric flow	231 m^3/s
SO_X	236 mg/m^3
NO_X	1004 mg/m^3
CO_2	14-16.5%
O_2	2.5-5%
40% excess air was supplied to boiler for combustion of coal	

Table 4 Chemical and physical analyses of coal used in test boiler

Constituent	Wt.%
Total moisture (inherent + surface)	10.43
Inherent moisture	7.55
Ash	34.74
Ash on fire basis (actual)	33.64
Volatile matter	21.59
GC_v (Gross calorific value) in Kcal/kg	4187
GC_v on fire basis in Kcal/kg	4055
Net GC_v in Kcal/kg	3834
Unburnt carbon in fly ash	1.35
Unburnt carbon in bottom ash	5.75

mirror polished down to 1 μm alumina polishing on cloth wheel before performing tests. A hole of 2-mm diameter was drilled in each sample so as to hang the same in the boiler at a selected location. Obviously, the direction of the gas stream containing fly ash particles is different at different locations in the boilers, which may vary from vertical to horizontal, downward to upward or inclined depending upon the orientation of boiler/superheater tubes. Therefore, a particular location was identified in the boiler unit III of the plant to hang the samples as per the recommendation of the plant authorities. At this particular location, a comparatively highly aggressive condition of flow exists, and some severe failures due to erosion have been noticed by the concerned power plant in this zone. The samples were inserted in the boiler with the help of stainless steel wire through the soot blower dummy points at 41-m height from the base of the boiler. The temperature of the hanging zone was about 700 ± 10 °C with full load of 210 MW. The direction of gas flow is vertically downward in this zone. The velocity of the gas stream was 13 m/s. As the samples were coated from all sides and were hung with the help of nichrome wires, the angle of the gas stream impingement at the top edge of the surface was 90°, whereas on the other four edges (two major flat surfaces as well), the gas stream went parallel. At the bottom of the samples, no gas stream was present. It is pertinent to mention that it is not possible to comment on the direction of impingement of the particles of the gas stream, due to which each surface is receiving eroding particles with different impingement angles at various locations. In this sense, the erosion conditions can be regarded as highly randomized with turbulent gas flow. It was not possible even to monitor in the given environment. The samples were exposed for 15 cycles, each cycle consisting of 100-h exposure in the boiler and 1 h cooling in air. The mass change data were taken after each cycle along with physical observations to approximate the kinetics of E-C. However, in this environment, the mass change data alone could not be of much use for predicting E-C behavior because of suspected spalling and ash deposition on the samples. Therefore, the extent of E-C has also been evaluated by measuring the thickness of the scale lost due to erosion, spalling, or evaporation by finding the difference in thickness of the specimens before and after 1500-h exposure to the actual environment. The thickness was measured using a Sylvac micrometer screw gauge (Swiss make, resolution 0.001), and represented value was taken as the average of three measured values. Before the thickness measurements, the specimens were cleaned properly with a gentle brush to remove any ash or loose contaminants, etc. X-ray diffraction analysis (XRD) of the exposed samples was performed. SEM/EDS analysis was done for the surface as well as of the cross sections of the exposed samples as per the procedure given in section 2.2. The scale in this study has been referred to as the material present above the substrate steel, which may include oxidized/partially oxidized/unaffected coating layers plus any other layer found on the surface, as could be seen from the cross-sectional micrographs. The assumption was made because, after the exposure, every coating may suffer some internal oxidation to different depths which is usually not easy to measure.

3. Results

3.1 Visual Observations, Thickness, and Porosity

The bare substrate was lustrous gray in color. The D-Gun-sprayed Ni-20Cr was dark gray in color. The thickness of the coatings has been measured from the Back Scattered Electron Images (BSEI) (Fig. 1) and was found to be 110 μm. Average apparent surface porosity of the coating was found to be 1.3%.

3.2 XRD Analysis

The XRD diffraction patterns of the Ni-20Cr coating in as-sprayed condition are depicted in Fig. 2. The analysis

indicates the presence of Ni as the principal phase in the coating, thereby predicting the formation of γ-Ni solid solution.

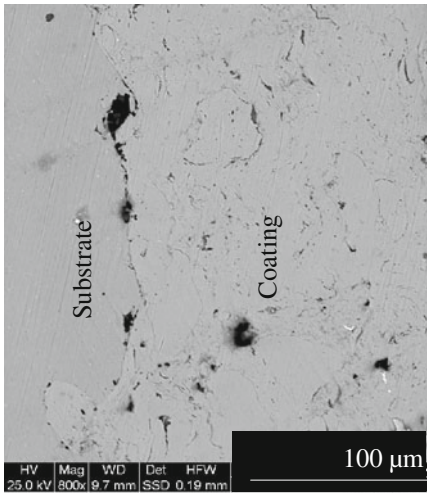

Fig. 1 BSEI showing the cross-sectional morphology of D-Gun-sprayed Ni-20Cr coating on 347H boiler steel by FE-SEM

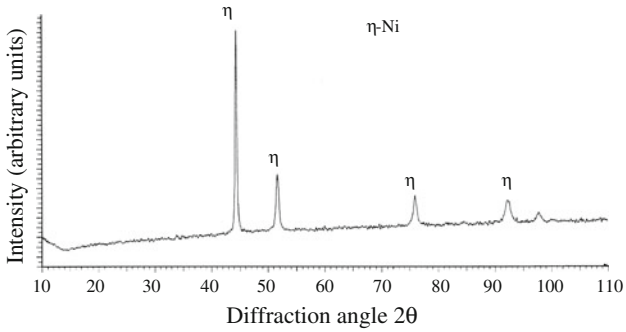

Fig. 2 X-ray diffraction profiles of the D-Gun-sprayed Ni-20Cr coating on 347H boiler steel

3.3 SEM/EDS Analysis of As-Sprayed Coating

3.3.1 Surface Analysis. The surface scale morphologies of the D-Gun-sprayed Ni-20Cr coating has been

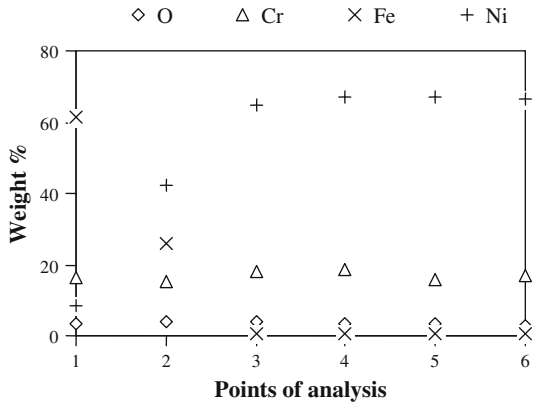

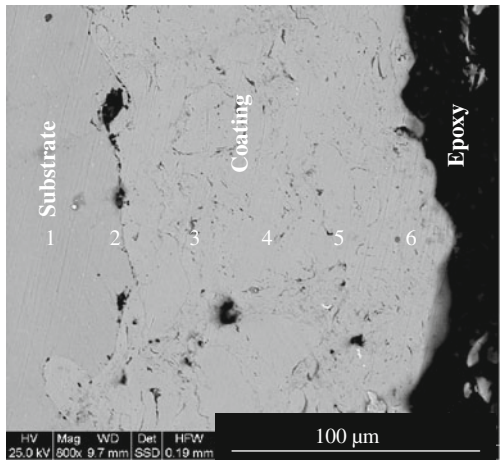

Fig. 4 Cross-sectional morphology and variation of elemental composition across the cross section of D-Gun-sprayed Ni-20Cr coating on 347H boiler steel

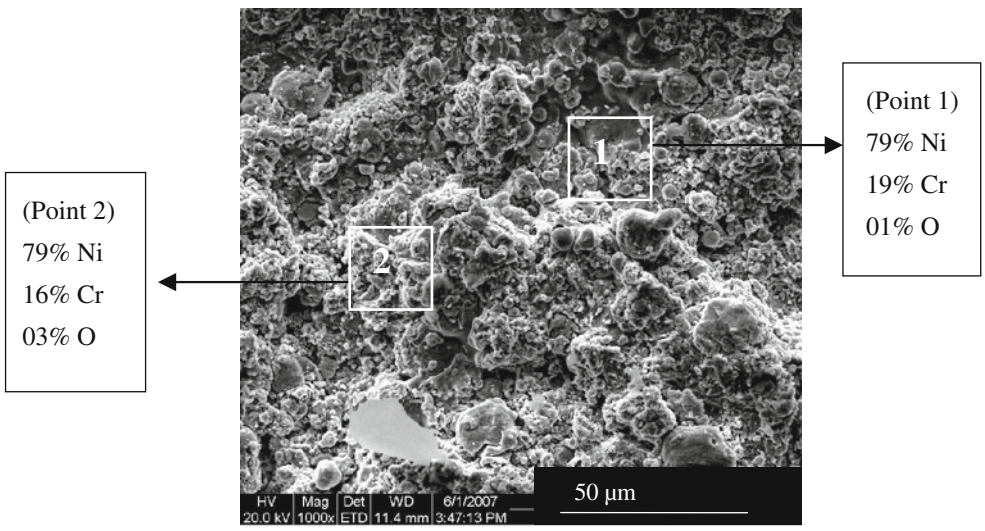

Fig. 3 EDS analysis of the D-Gun-sprayed Ni-20Cr coating on surface

reported in Fig. 3. The microstructure of the coating is composed of fine globular particles. The EDS analysis at points 1 and 2 indicate the presence of mainly Ni and Cr along with minor amounts of O. The EDS analysis of the coating surface shows that the compositions of the scales at points 1 and 2 are nearly similar and are also approaching to that of the feedstock powder. The gray-colored filled area is possibly some external contamination that might have been left on the sample during analysis.

3.3.2 Cross-Sectional Analysis of As-Sprayed Coating. The cross-sectional SEM image of the D-Gun-sprayed Ni-20Cr coating on the 347H boiler steel is shown in Fig. 4. A uniform dense coating adherent with the base metal is observed in general. There is the presence of some voids in the coating microstructure; some of them are along coating/substrate interface. Some oxide stringers are also visible in the coating, which are mostly aligned in a laminar fashion.

3.3.3 X-Ray Mapping of As-Sprayed Coating. BSEI and x-ray mappings of the cross section of the as-sprayed substrate are shown in Fig. 5. It is evident from the maps that Fe is mainly confined to the base metal and the coating contains mainly Ni, whereas Cr is present in the coating as well in the base steel. Oxygen is mainly

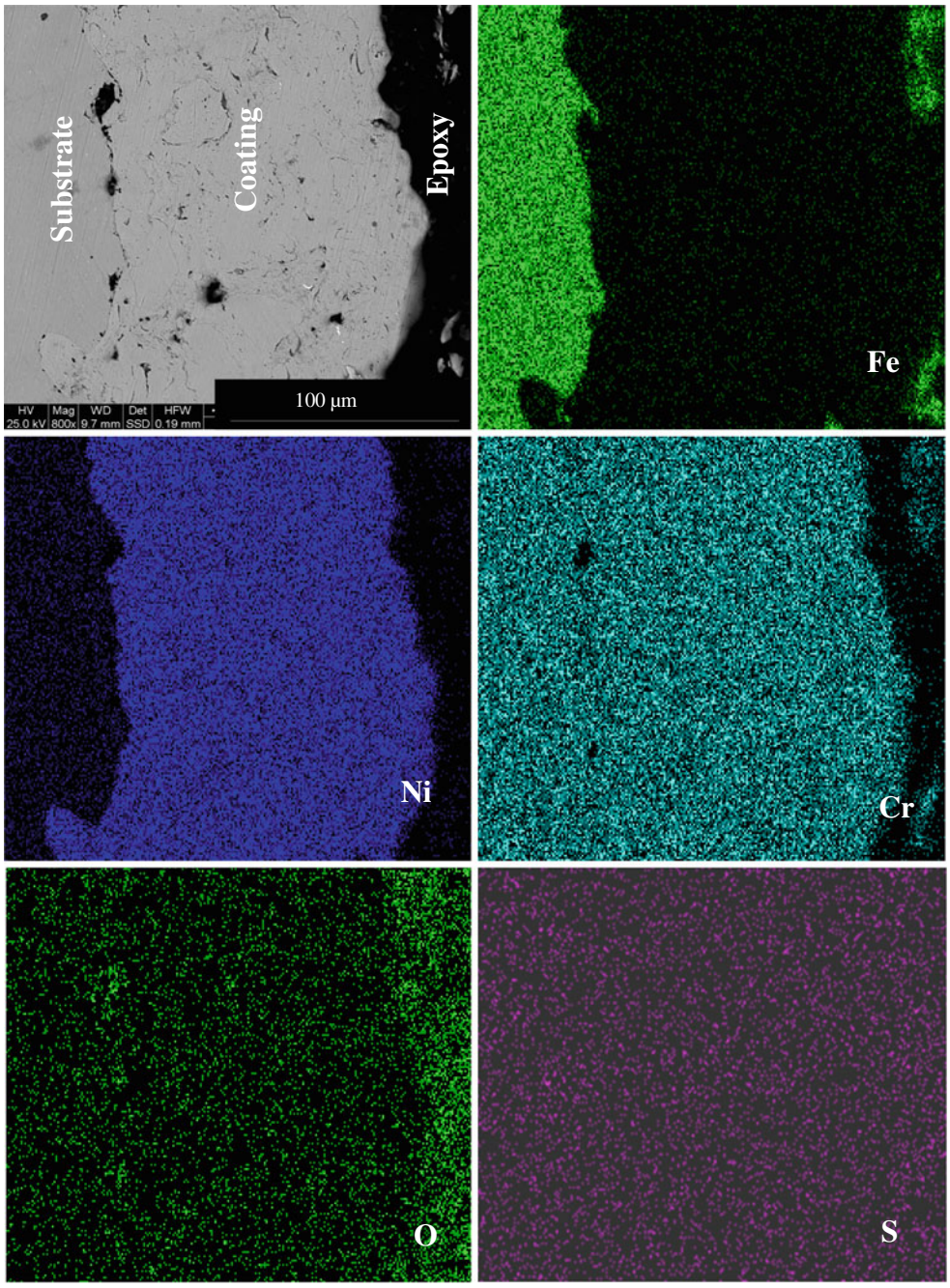

Fig. 5 BSEI and x-ray mappings of the cross section of the D-Gun-sprayed Ni-20Cr coating on 347H boiler steel

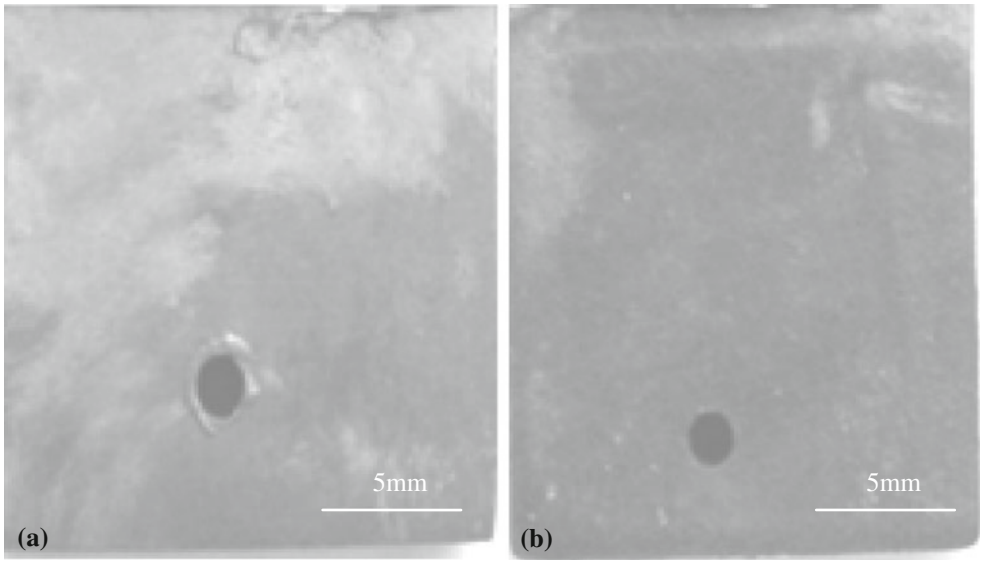

Fig. 6 Appearance of the uncoated (a) and Ni-20Cr D-Gun-spray-coated (b) specimens exposed to actual boiler conditions at 700 °C for 15 cycles

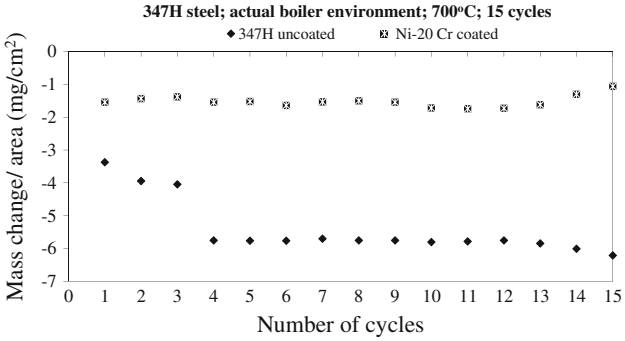

Fig. 7 Mass change with the number of exposure cycles for the uncoated and D-Gun-sprayed Ni-20Cr-coated 347H boiler steel by erosion-corrosion in actual boiler environment at 700 °C for 15 cycles

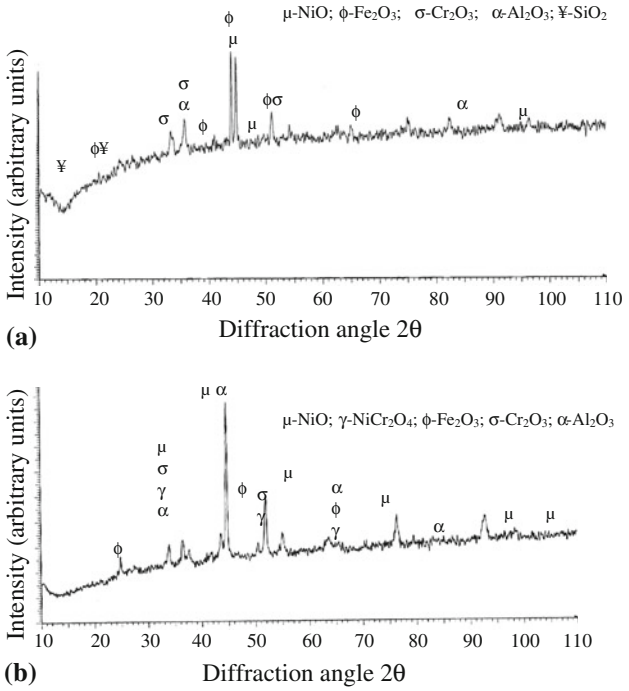

Fig. 8 X-ray diffraction profiles of the uncoated (a) and Ni-20Cr D-Gun spray-coated (b) 347H specimens exposed to actual boiler conditions at 700 °C for 15 cycles

observed in the top layers of the coating. Sulfur is seen in a scattered form.

3.4 Actual Environment

3.4.1 Visual Observations. The macrographs of exposed specimens are depicted in Fig. 6(a, b). The uncoated 347H steel changed its color after the completion of the second cycle from lustrous gray to dull gray. Subsequently, the color of sample turned to black gray by the completion of the study. 347H steel changed its color from lustrous gray to brown. The color of the sample further darkened with the progress of the experiment. However, no spallation of the scale was observed.

The Ni-20Cr-coated sample changed from dark gray to dull brown during the early cycles of study, and it continued to become darker toward blackish-brown appearance by the end of the cyclic studies. No visible cracks were observed on the surfaces of the coating, and the coating did not show any spallation tendency. The scales formed on the coated samples were found to be intact even after the 15th cycle of the exposure.

3.4.2 Kinetics. Mass change data in mg/cm^2 as a function of time expressed in hours for the uncoated and Ni-20Cr-coated 347H boiler steel after exposure in actual environment are compiled in Fig. 7. It can be observed from the mass change graphs that the mass losses have

taken place in the both cases, in the initial cycles; however after applying coating, the loss has been reduced. The initial mass losses may perhaps be due to the erosion, or there has been a formation of some volatile species, which escaped from the steel surfaces. However, the probability of the latter is marginal at the working temperature of 700 °C. The uncoated 347H steel has shown mass loss amounting to 6.21 mg/cm^2, whereas after the deposition of the D-Gun-sprayed Ni-20Cr coating, the mass loss was reduced to 1.06 mg/cm^2. The overall mass loss for the 347H steel has reduced by 83% after the deposition of the Ni-20Cr coating.The extent of EC has been measured in terms of metal lost after 1500 h of exposure, after proper cleaning of the samples. The thickness loss for the uncoated substrate was 0.19 mm, and it was reduced to 0.09 mm after the deposition of the coating.The corresponding degradation rates expressed in mils per year is found to be 43 mpy (1.10 mm/year) for uncoated substrate and 20 mpy (0.52 mm/year) for the coated substrate.

3.4.3 XRD Analysis of the Exposed Specimen. The XRD patterns of the exposed specimens are depicted in Fig. 8(a, b). The uncoated 347H has NiO, Fe_2O_3, and Al_2O_3 as main phases. Some phases of Cr_2O_3 and SiO_2 are also observed. On the contrary, the D-Gun-spray Ni-20Cr-coated 347H substrate has a strong presence of NiO phase along with Cr_2O_3 phase. Some other phases, such as $NiCr_2O_4$, Fe_2O_3, and Al_2O_3, are also revealed. The presence of Al_2O_3 phase may be due to the deposition of ash particles in the outer layer of scale.

3.4.4 SEM/EDS of Exposed Samples. Surface *Analysis:* The surface scale morphologies of the uncoated 347H steel and D-Gun-sprayed Ni-20Cr coatings subjected to actual boiler conditions are reported in Fig. 9(a) and (b), respectively. The oxide scale of the 347H steel (Fig. 9a) consists of an upper sub-layer dispersed in the matrix. The sub-layer is in the form of patches, which are surrounded by low-lying channels. Some spherical particles are seen dispersed in these low-lying channels. Furthermore, the EDS analysis of these particles corresponding to point 1 indicates that these particles are mostly ash particles, which might have deposited during the exposure. The EDS composition at point 2 indicates that the oxide scale is mainly consisting of Fe and O, thereby indicating the formation of Fe_2O_3-rich oxide scale on the steel.

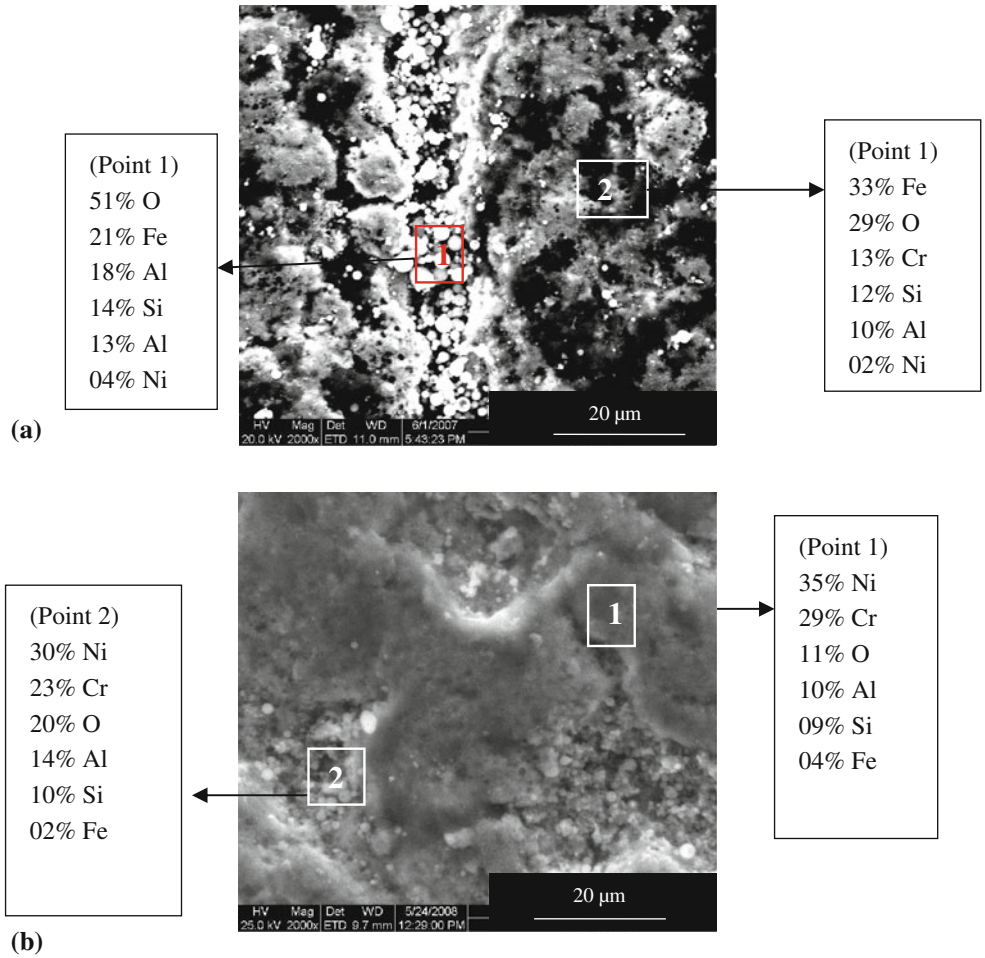

Fig. 9 EDS analysis of the uncoated (a) and D-Gun-sprayed Ni-20Cr-coated (b) 347H steel exposed to actual boiler conditions at 700 °C for 15 cycles

The Ni-20Cr coating (Fig. 9b) reveals that localized regions at the surface exhibit distinct scaling behavior. The oxide scale, by and large, has a dense morphology, whereas fine-grained particles are seen in some of the areas of the scale with some patches. The dense part mainly represents the coating which is rich in Ni, Cr, and O. The patches have slightly more of Al and Si (refer point 2).

Cross-Sectional *Analysis:* The BSE image indicating oxide scale morphology and corresponding EDS analysis at some selected points across the cross section of the Ni-20Cr-coated 347H substrate after exposure to platen superheater of the coal fired boiler is shown in Fig. 10. The scale seems well adherent with the base steel. The base metal elements are restricted up to the interface point 2; the scale of specimen is found to have significant amount of Ni in addition to appreciable amounts of Cr along its thickness as is evident from the EDS composition at points 2 and 6. There is only marginal penetration of oxygen along the thickness of the scale.

X-Ray *Mappings of Exposed Specimens:* BSEI and x-ray mappings of the cross section of the uncoated 347H boiler steel after subjected to cyclic conditions in the actual boiler for 1500 h are shown in Fig. 11. The elemental maps mainly show Fe and Cr in the base metal as well as in the outer scale. Aluminum is also found in the outer layers. The x-ray mapping of the exposed Ni-20Cr-coated specimen (Fig. 12) reveals that Fe is mainly confined to base metal. The oxide scale consists mainly of Ni. A thick layer of Cr can be seen along with O in the outer regions of the scale indicating the probable formation of outermost protective Cr_2O_3 layer. Silicon is also seen in the top layers of the scale. Sulfur is rarely seen.

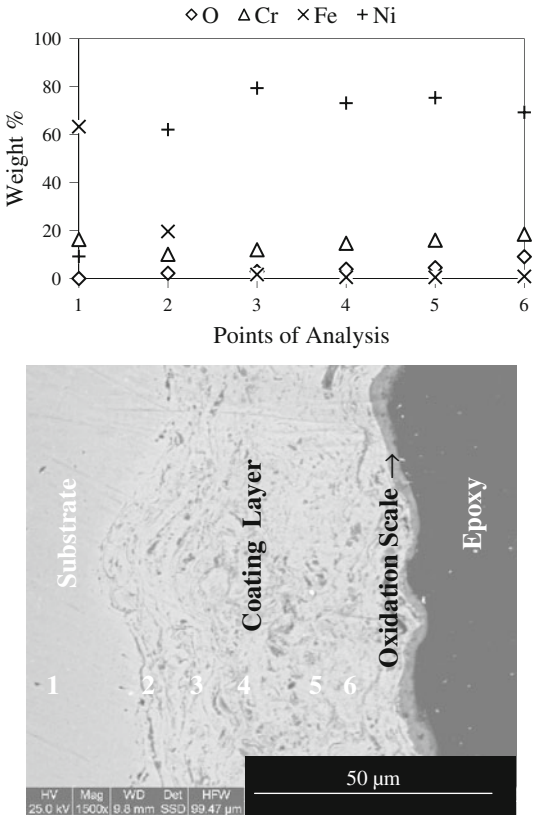

Fig. 10 Cross-sectional morphology and variation of elemental composition in the cross section of the D-Gun-sprayed Ni-20Cr-coated boiler steel exposed to actual boiler environment for 15 cycles

4. Discussions

The Ni-20Cr coating was successfully coated on the chosen 347H boiler substrate steel by the D-Gun-sprayed method at the given process parameters. The coating of about 110 µm was obtained on the given steel. It is learnt that the coatings should have minimum possible porosities because high values can do harm to the persistent E-C resistance of thermal spray coatings. The porosity of the D-Gun coating has been found to be low with an average value of 1.3% which seems to be acceptable from the point of view of E-C protection. The measured value of porosity is in good agreement with the earlier studies (Ref 20, 21). X-ray diffractogram for the D-Gun-sprayed Ni-20Cr coating has confirmed the presence of higher amounts of Ni, as the primary phase which is consistent with powder composition (80Ni and 20Cr). This observation is in good agreement with the phases reported by Ak et al. (Ref 22). The XRD result is further endorsed by the EDS analysis, which shows the dominating presence of of Ni and Cr in the coating. The microstructure of the D-Gun-sprayed coating appeared to be dense and generally free of oxide particle inclusions, as the amount of oxygen is marginal (Fig. 3), which is supported by corresponding x-ray mapping analysis (Fig. 5). The coating-substrate interface is found to be intact and continuous. The coating elements are restricted to the coating region. The elements identified by the cross-sectional EDS analysis are further supplemented by the corresponding x-ray mappings. The mappings indicated rich presence of Ni and Cr in the as-sprayed D-Gun-sprayed coating. It has also been observed from the x-ray mappings that the inter-diffusion of various elements between the substrate and the D-Gun-sprayed coating, in general, is found to be marginal.

During the exposure in the actual boiler environment, overall mass loss has been indicated in both the cases, but mass loss was appreciably reduced after the application of Ni-20Cr coating. The overall E-C loss of the alloy reduced by 83% after the deposition of the coating. It has been observed that the E-C mass losses took place only during the initial four cycles (may be defined as transient period of E-C) of exposure in the boiler environment for both the coatings. This behavior may be attributed to the erosion of micro-hills present on the coated samples. However, once the surfaces of the samples became smooth, no further erosion took place, and the process achieved steady-state

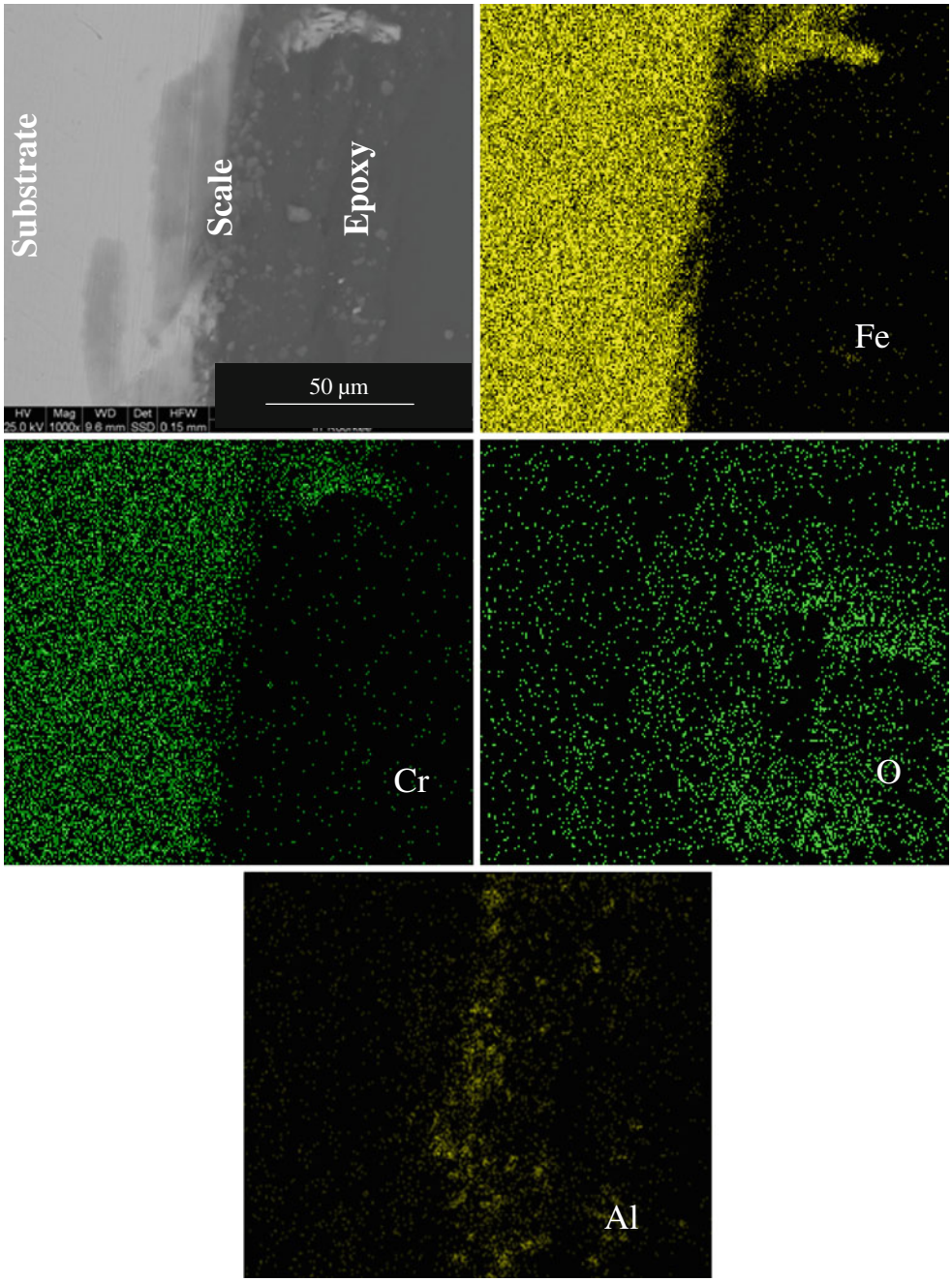

Fig. 11 BSEI and x-ray mapping of the cross section of the uncoated 347H boiler steel exposed to actual boiler conditions at 700 °C for 15 cycles

conditions. The role of the coating is pronounced during the transient period of erosion during, which saved the substrate steel from incurring the enhanced E-C loss. The mass losses recorded after the initial transient cycles for both the coatings were meager, which indicates that the coatings could be beneficial to reduce the E-C of the substrate steel during longer exposures in the actual boiler environment. Furthermore, the degradation rate in terms of thickness has reduced to 20 mpy from 43 mpy after the deposition of the coating.

The SEM/EDS analysis has revealed appreciable amount of Fe in the top oxide scale of the uncoated steel when subjected to actual boiler conditions, which may be attributed to the fact that Fe might have diffused from the bulk metal. This is further supported by the surface XRD analysis of the uncoated substrate in the form of formation of Fe_2O_3 as the main constituent of the top scale, which indicates the onset of oxidation as well. The formation of Fe_2O_3 in the scale has been reported to be non-protective by Das et al. (Ref 23). However, the coating is found to

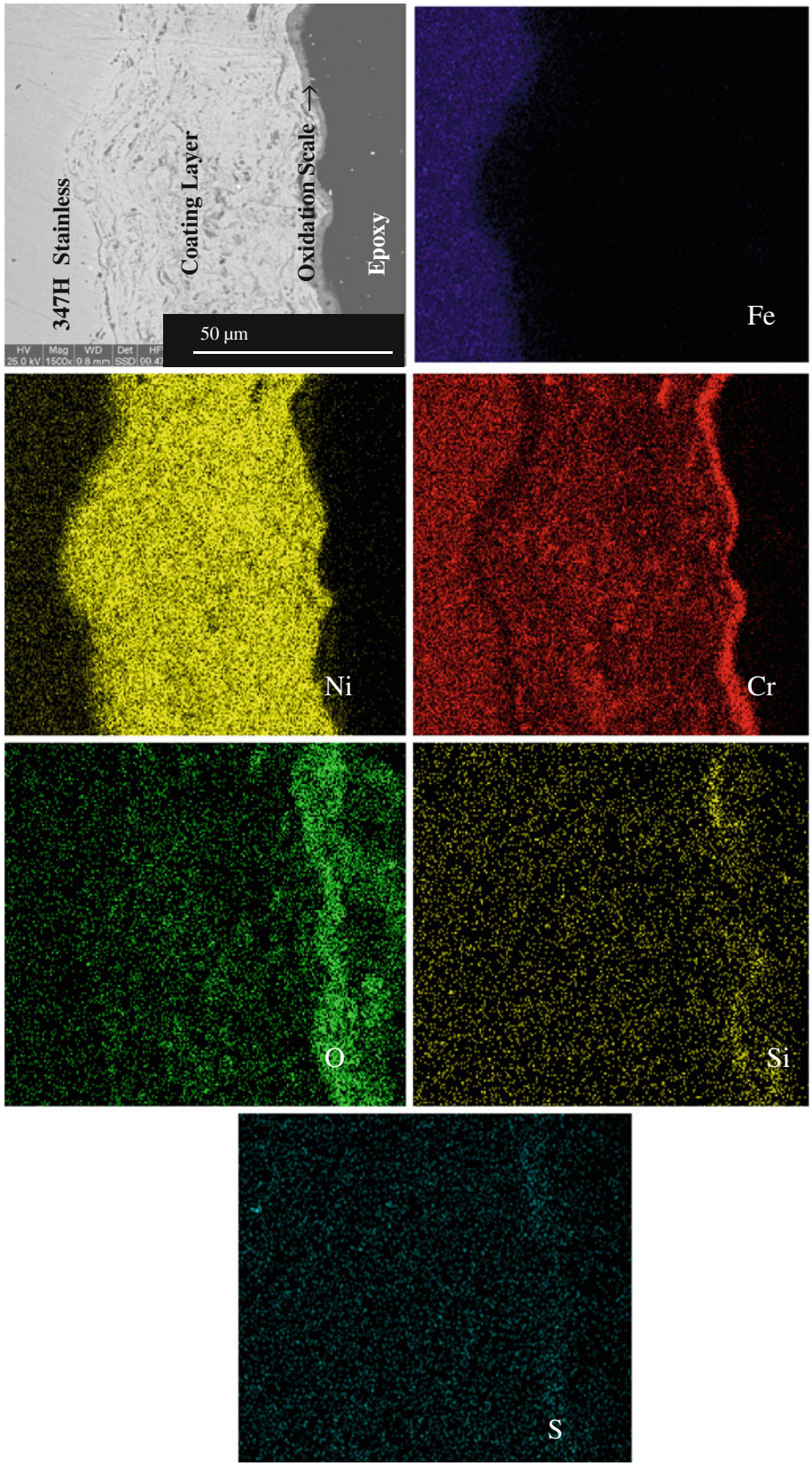

Fig. 12 BSEI and x-ray mapping of the cross section of the D-Gun-sprayed Ni-20Cr-coated 347H boiler steel exposed to actual boiler conditions at 700 °C for 15 cycles

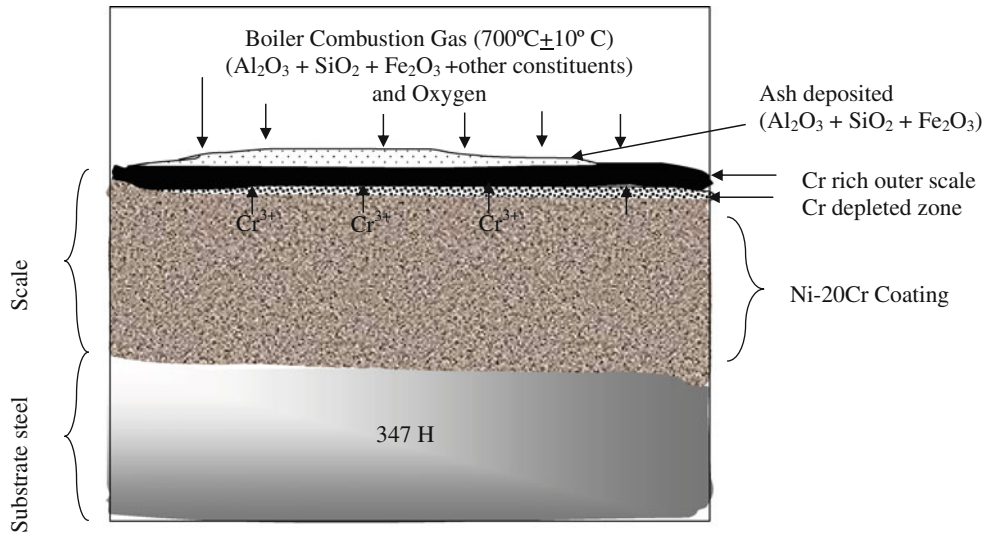

Fig. 13 Schematic diagram illustrating the surface structure mode of the D-Gun-sprayed Ni-20Cr coating layer after exposure to boiler environment

have retained its identity even after E-C testing under cyclic conditions (Fig. 10). The figure further indicates that the coating has been successful to retain its continuous surface contact with the substrate steel, even after the exposure. The concentration of Ni is decreasing gradually beyond the point 3, whereas that of Cr is increasing beyond this point with maxima at point 6. Oxygen is also seen in high amount at point 6, which indicates the probable formation of an outermost chromium oxide layer on the scale. This is further endorsed by the x-ray mapping analysis reported in Fig. 12, showing that the coating mainly consists of Ni, with a significant presence of Cr. The outermost layer of the exposed coating contains mainly Cr along with O, thereby indicating the possibility of formation of Cr_2O_3. The XRD analysis (Fig. 8b) further endorsed the formation of Cr_2O_3 in the eroded-corroded coating. The chromium oxide phase is thermodynamically stable (Ref 24) up to very high temperatures because of its high melting points as well as because it forms a dense, continuous, and adherent layers that grow relatively slowly (Ref 25). The scale of this type forms a solid diffusion barrier that inhibits interaction of oxygen of underlying coating. For the coating, the dispersed Cr-particles promoted selective oxidation to form a dense Cr_2O_3 film with fine grain structure. This phase is an oxidation protective phase along with its adequate hardness to avoid the E-C of the substrate steel. Besides, the presence of a spinel phase ($NiCr_2O_4$) in the oxide scale of the coated steel may further enhance the corrosion resistance, because the spinel phases have much lower diffusion coefficients of their cations and anions than those in the parent oxide phases (Ref 26).

It has been reported that sigma (σ) phase is hard and fragile; in addition, when it forms, it consumes chromium and molybdenum present within the matrix (Ref 27), which leads to the depletion in these elements, and thereby prevents formation of Cr_2O_3. XRD analysis of the exposed coated specimen tested in the given environments indicated that no brittle (σ) phase was formed in the scales. Cross-sectional analysis and x-ray mappings, in general, revealed minor interdiffusion of various elements between the substrate and the D-Gun-sprayed coating. Minor interdiffusion is reported to be beneficial (Ref 28) for providing better adhesion between the substrate and the coating.

So far as simultaneous oxidation of the coating along with its erosion is concerned during the exposure, the oxidation of the coating is limited only to the upper layers. The analysis has shown the formation of oxides of Ni and Cr in upper layers. This is evident from x-ray mappings of the eroded-corroded coating where oxygen is mainly limited to the upper layers of the coating. This is further endorsed by the cross-sectional SEM-EDS analysis (Fig. 10), where oxygen is found in substantial amounts only in outer layer at point 6. Once the Cr_2O_3-rich scale is formed on the sample surface, it inhibits the further diffusion of oxidizing species into the coating layers.

Some globular particles in the microstructures of the eroded-corroded samples have their composition similar to that of the chemical analysis of the ash present in the boiler environment (Refer Table 2). Evidently, these globular particles represent the ash particles retained on the surfaces of the samples during the exposure. Based on the results and observations of the study, a schematic diagram (Fig. 13) has been proposed to illustrate the E-C mode for the coating. As is clear from the figure, there is an outermost layer that contains mainly the ash particles getting deposited from the boiler environment. Followed by this, a thin chromia layer, is formed by outward diffusion of the chromium from the coating region and inward diffusion of O from the environment. The outward diffusion of Cr is evident from the presence of a Cr-depleted inner layer just below the thin Cr-rich layer. The inner scale is mainly composed of Ni and Cr layers.

5. Conclusions

- The Ni-20Cr powder could be successfully sprayed on 347H boiler steel by the D-Gun-spraying process.
- The uncoated 347H boiler steel showed intensive E-C in the form of mass as well as thickness loss during tests which was reduced appreciably to a low value by the application of the coatings. The coating was found to be successful in reducing mass loss by 83% as well as thickness loss by 53%, thereby indicating good E-C resistance.
- The improved E-C resistance of the Ni-20Cr coating could be attributed to the formation of Cr-rich outer scale subsequent upon the exposure to the actual boiler environment.
- The oxidation of the coating was limited to some of its upper layers.

Acknowledgments

The authors thankfully acknowledge the research grant from the Department of Science and Technology, Ministry of Science and Technology, New Delhi under SERC Fast Track Proposal for Young Scientists Scheme (File No. SR/FTP/ETA-06/06, dated March 16, 2006) for carrying out the R&D study on ''Development of erosion-corrosion resistant thermal spray coatings for the power plant boilers''.

References

1. A.J. Cuttler, Fire-Side Corrosion in Power Station Boilers, CEGB Research Report, 1978
2. B.Q. Wang and K. Luer, The Relative Erosion-Corrosion Resistance of Commercial Thermal Spray Coatings in a Simulated Circulating Fluidized Bed Combustor Environment, *Proceedings of 7th National Thermal Spray Conference*, June 20-24, 1994 (Boston, MA), p 115-120
3. R.A. Rapp, Chemistry and Electrochemistry of the Hot Corrosion of Metals, *Corrosion*, 1986, **42**(10), p 568-577
4. G. Sorell and C.M. Schillmoller, Alloys for High Temperature Service in Municipal Waste Incinerators, *ASM First International Conference on Heat-Resistant Materials* (Lake Geneva, Wisconsin, USA), 1991
5. W. Nelson and C. Cain, Corrosion of Superheaters and Reheaters of Pulverized Coal Fired Boilers, *Trans. ASME J. Eng. Power*, 1960, **82**, p 194-204
6. R. Backman, M. Hupa, and E. Uppstu, Fouling and Corrosion Mechanisms in the Recovery Boiler Superheater Area, *TAPPI J.*, 1986, **70**(6), p 123-132
7. V.H. Hidalgo, J.B. Varela, A.C. Menendez, and S.P. Martinez, High Temperature Erosion Wear of Flames and Plasma-sprayed Nickel-Chromium Coatings Under Coal-Fired Boiler Atmospheres, *Wear*, 2001, **247**, p 222-241
8. N. Eliaz, G. Shemeshand, and R.M. Latanision, Hot Corrosion in Gas Turbine Components, *Eng. Fail. Anal.*, 2002, **9**, p 31-43
9. T. Sundararajan, S. Kuroda, T. Itagaki, and F. Abe, Steam Oxidation Resistance of Ni-Cr Thermal Spray Coatings on 9Cr-1Mo Steel. Part 1: 80Ni-20Cr, *ISIJ Int.*, 2003, **43**(1), p 95-103
10. T. Sundararajan, S. Kuroda, T. Itagaki, and F. Abe, Steam Oxidation Studies on 50Ni-50Cr HVOF Coatings on 9Cr-1Mo Steel: Change in Structure and Morphology Across the Coating/Substrate Interface, *Mater. Trans.*, 2004, **45**(4), p 1299-1305
11. Y. Matsubara and A. Tomiguchi, Surface Texture and Adhesive Strength of High Velocity Oxy-Fuel Sprayed Coatings for Rolls of Steel Mills, *Proceedings of 13th International Thermal Spray Conference* (Florida, USA, 1992), p. 637-645
12. L. Byrnes and M. Kramer, Method and Apparatus for the Application of Thermal Spray Coatings onto Aluminium Engine Cylinder Bores, *Proceedings of the 7th National Thermal Spray Conference* (Boston, 1994), p 39-48
13. Y.J. Zhang, X.F. Sun, Y.C. Zhang, T. Jin, C.G. Deng, H.R. Guan, and Z.Q. Hu, A Comparative Study of DS NiCrAlY Coating and LPPS NiCrAlY Coating, *Mater. Sci. Eng.*, 2003, **360**, p 65-69
14. Metals Handbook, *Failure Analysis and Prevention*, vol. 10, ASM Publication, Metals Park OH, 1975
15. S. Prakash, B.S. Sidhu and A. Madeshia, Tube Failures in Coal Fired Boilers, *Proceedings of National Seminar on Advances in Material and Processing*, November 9-10, 2001 (IITR, Roorkee, India, 2001), p 245-253
16. S.D. Sullivan and F.M. Lewis, Combining Dual-Fuel Capability with Environmental Compliance, *FPAC Heating, Piping, Air Conditioning Engineering*, 2002, **74**, p 43-48
17. G. Kaushal, H. Singh, and S. Prakash, Comparative High Temperature Analysis of HVOF Sprayed and Detonation Gun Sprayed Ni-20Cr Coating in Laboratory and Actual Boiler Environments, *Oxid. Met.*, 2011, **76**(3-4), p 169-191
18. G. Kaushal, H. Singh, and S. Prakash, Surface Engineering of ASTM A213 TP 347H Steel to Enhance Its High Temperature Corrosion Resistance by Detonation-Gun Spray Coating, *Mater. High Temp.*, 2011, **28**(1), p 1-11
19. G. Kaushal, H. Singh, and S. Prakash, Role of HVOF Spray NiCr Coatings to Control High Temperature Oxidation of Boiler Steels, *International Thermal Spray Conference and Exposition, (ITSC 08)*, June 2-4 (Maastricht, The Netherlands, 2008), p 1351-1356
20. B. Rajasekaran, S.G.S. Raman, S.V. Joshi, and S. Sundararajan, Effect of Detonation Gun SPRAYED Cu-Ni-In Coating on Plain Fatigue and Fretting Fatigue Behaviour of Al-Mg-Si Alloy, *Surf. Coat. Technol.*, 2006, **201**(3-4), p 1548-1558
21. Y.A. Kharlamov, Detonation Spraying of Protective Coatings, *Mater. Sci. Eng.*, 1987, **93**, p 1-37
22. N.K. Ak, C. Tekmen, I. Ozdemir, H.S. Soykan, and E. Celik, NiCr Coatings on Stainless Steel by HVOF Technique, *Surf. Coat. Technol.*, 2003, **173-174**, p 1070-1073
23. D. Das, R. Balasubramaniam, and M.N. Mungole, Hot corrosion of Fe_3Al, *J. Mater. Sci.*, 2002, **37**(6), p 1135-1142
24. S. Kamal, R. Jayaganthan, S. Prakash, and S. Kumar, Hot Corrosion Behavior of Detonation Gun Sprayed Cr_3C_2-NiCr Coatings on Ni and Fe-Based Superalloys in Na_2SO_4-60%V_2O_5 Environment at 900°C, *J. Alloys Compd.*, 2008, **463**(1-2), p 358-372
25. F.H. Stott, Principles of Growth and Adhesion of Oxide Scales, *The Role of Active Elements in the Oxidation Behaviour of High Temperature Metals and Alloys*, E. Lang, Ed., Elsevier Applied Science, London, 1998
26. U.K. Chatterjee, S.K. Bose, and S.K. Roy, *Environmental Degradation of Metals*, Marcel Dekker, New York, 2001
27. A.M. Babakr, A. Al-Ahmari, K. Al-Jumayiah, and F. Habiby, Sigma Phase Formation and Embrittlement of Cast Iron-Chromium-Nickel (Fe-Cr-Ni) Alloys, *J. Miner. Mater. Charact. Eng.*, 2008, **7**(2), p 127-145
28. J.R. Nicholls, Designing Oxidation-Resistant Coatings, *JOM*, 2000, **52**, p 28-35